

## Laurdan Generalized Polarization: from cuvette to microscope

S. A. Sanchez<sup>\*1</sup>, M.A. Tricerri<sup>2</sup>, G. Gunther<sup>3</sup> and E. Gratton<sup>1</sup>

<sup>1</sup>Laboratory for Fluorescence Dynamics, University of California at Irvine, CA, USA

<sup>2</sup>Instituto de Investigaciones Bioquímicas de La Plata (INIBIOLP). Fac. Cs. Médicas, Universidad Nacional de La Plata, La Plata, Argentina.

<sup>3</sup>Laboratorio de Cinética y Fotoquímica, Facultad de Ciencias Químicas y Farmacéuticas, Universidad de Chile, Santiago, Chile.

Laurdan is a fluorescent molecule that detects changes in membrane phase properties through its sensitivity to the polarity of the environment in the bilayer. Polarity changes are shown by shifts in the Laurdan emission spectrum, which are quantified by calculating the generalized polarization (GP). This technique was originally developed to be used in a cuvette fluorometer. With the development of two-photon microscopy, Laurdan GP has evolved into a technique capable of spatially resolve micro-domains of different solvent penetration. We discuss here the basic concepts, instrumentation and experimental considerations when transferring the GP technique from the cuvette to the microscope. We also discuss examples of Laurdan GP in membrane model systems using both cuvette and microscope approaches to compare the two methodologies.

**Keywords** Laurdan, GUVs, two-photon excitation microscopy, Laurdan General Polarization imaging.

### 1. Introduction

Fluorescence techniques such as fluorescence lifetime or simple intensity measurements were originally developed to be used in a cuvette fluorometer. The implementation of these techniques in the microscope platform added the spatial resolution needed for cellular studies, but also forced researchers to change the experimental design, systems and the analytical methods used. One of these techniques, Laurdan Generalized Polarization and its transition from the cuvette to the microscope, is the focus of this report. Laurdan (6-lauroyl,1,2-dimethylamino naphthalene) is a fluorescent dye designed and synthesized in 1979 by Gregorio Weber [1] to study the phenomenon of dipolar relaxation. Polarity changes are detected by shifts in the Laurdan emission spectrum, and the Generalized Polarization function (GP) was defined as a way of measuring wavelength displacements [2]. Changes in GP values when lipid bilayers are either in fluid or gel phase extended the use of the technique to the field of membrane dynamics and protein-lipid interaction [2]. Articles using GP measurements in cuvette go from *in vitro* studies like lipid characterization [3,4], cholesterol [5,6] and detergent [7] effects in lipid phases, lipid- protein interaction [8-10], effect of hydrostatic pressure on membrane protein activity [11], to *in vivo* studies like the effect of drugs in lipid packing [12] and membrane susceptibility to PLA<sub>2</sub> [13]

In 1997 GP measurements were done for the first time in the microscope using two-photon excitation to minimize photobleaching of the dye [14]. Microscopy added to the GP technique the submicron spatial resolution critical for cellular studies, as exemplified by recent reports on the visualization of membrane packing and lipid domains both *in vitro* [15-20] and *in vivo* [21-23]. Here we explain the basic concepts of the technique both in cuvette and in the microscope and show examples how microscopic GP measurements give valuable information that cannot be obtained from cuvette measurements.

---

\* Corresponding author: e-mail: susanas@uci.edu

## 2. Laurdan structure and spectral shift

The fluorescent naphthalene moiety of the Laurdan molecule (Figure 1a) possesses a dipole moment due to a partial charge separation between the 2-dimethylamino and the 6-carbonyl residues. This dipole moment increases upon excitation and may cause reorientation of the surrounding solvent dipoles. The energy required for solvent reorientation decreases the excited state energy of the probe, which is reflected in a continuous red shift of the probe's emission spectrum. A schematic diagram of this relaxation process is given in Figure 1b. A blue-shifted emission is observed in apolar solvents, while a red-shifted emission is observed in polar solvents.

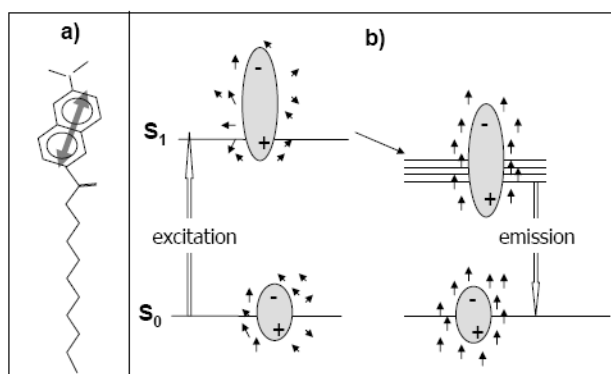


**Fig.1** a) Laurdan molecule dipole moment (grey arrow) created by the partial charge separation between the 2-dimethylamino and the 6-carbonyl residues. b) Diagram showing the changes in the Laurdan dipolar moment (in grey) after excitation from the ground state ( $S_0$ ) and later relaxation from  $S_1$ . The red shift of the spectra occurs when water molecules around the Laurdan molecules (arrows) reorganize to account for the Laurdan dipole increase after excitation.

One application of the spectral shift of Laurdan is the study of lipid bilayers. The hydrophobic tail of the lauric fatty acid allows solubilization of the probe within phospholipid bilayers, locating the fluorescent moiety toward the aqueous environment. When the lipids are in a gel-phase, the emission maximum of Laurdan is centered on 440 nm and when the lipids are in a liquid-crystalline phase the emission maximum is centered at 490 nm. This spectral shift is the result of the dipolar relaxation of Laurdan on the lipidic environment. The origin of this dipolar relaxation has been attributed to a few water molecules present in the bilayer at the level of the glycerol backbone, where the Laurdan naphthalene moiety resides (Figure 2) [4]. The concentration and molecular dynamics of these water molecules is a function of the phospholipid phase state, where water reorientation along the probe excited-state dipole occurs only in the liquid-crystalline phase.

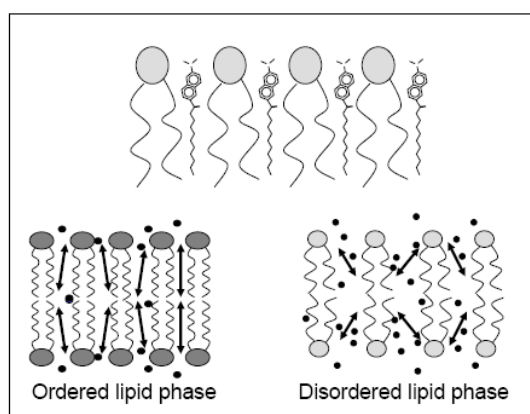


**Fig. 2** Naphthalene moiety of Laurdan locates in the membrane at the level of the glycerol backbone of the phospholipids. The rearrangement of few water molecules (black dots) localized around the Laurdan dipole (arrows) will be responsible for the red shift observed in different phases.

### 3. Laurdan GP and membrane studies in the cuvette

The shift of the emission maximum of Laurdan can be quantified by the Generalized Polarization (GP) function defined as [2]

$$GP = \frac{I_{440} - I_{490}}{I_{440} + I_{490}} \quad (1)$$

where  $I_{440}$  and  $I_{490}$  are the emission intensities at 440 and 490 nm respectively. A full discussion on the use and mathematical significance of GP can be found in the literature [5,19].

Cuvette measurements of Laurdan GP are done in a conventional fluorometer using excitation light at 340-360 nm and by simply registering the two mentioned emission intensities. Laurdan is normally dissolved either in ethanol or DMSO (di-methyl sulphoxide) and added to the liposomes at a Laurdan:lipid molar ratio of 1:1000 to 1:300 keeping the concentration of the organic solvent low enough to avoid altering the biological samples. The more common lipid model systems used in this type of measurements are small (SUVs), large (LUVs) unilamellar or multilamellar (MLVs) vesicles or small cells such as erythrocytes that are kept from sedimentation to the bottom by constant stirring.

Figure 3a shows the emission spectra of Laurdan within multilamellar vesicles (MLVs) of DPPC (dipalmitoylphosphatidylcholine) at two temperatures: 50°C, where the lipid is in the liquid-crystalline phase and 35°C, where DPPC is in the gel phase. The GP value at each temperature can be determined using eq.1. By following the spectral shift as a function of temperature it is possible to determine the transition temperature ( $T_m$ ) for the lipid under study (Figure 3b). Theoretically the values for the GP function go from -1.0 to +1.0; however, experimentally they range from 0.6 to -0.3 [4] both for pure lipids and for mixtures. More specifically, depending on the lipid composition and temperature, GP in the liquid phase goes from 0.3 to -0.3 while the values for the gel phase are typically range from 0.5 to 0.6.

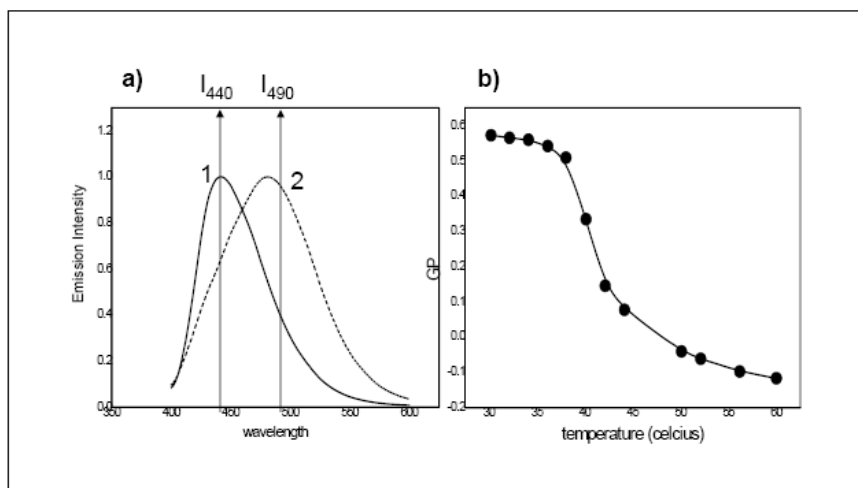


**Fig. 3** GP measurements in the cuvette. Laurdan emission spectrum is extremely sensitive to the degree of water penetration in the membrane. a) Emission spectra of Laurdan solubilized DPPC small unilamellar vesicles at 35°C (1) and 50°C (2). b) Changes of GP for DPPC with temperature,  $T_m$  equals 41°C.

#### 4. Laurdan GP imaging

Laurdan GP measurements in the microscope are done using two-photon excitation. Traditional one photon confocal excitation must be avoided because it induces severe photobleaching of the probe making it impossible to collect images under the confocal microscope for more than few seconds [19]. Two-photon excitation minimizes this problem due to the confined excitation volume that leaves the areas above and below the focal plane free of absorption, reducing the extent of probe photobleaching. An additional advantage of the small excitation volume is the intrinsic sectioning (confocal) effect that allows the researcher to collect images from different focal planes. Excellent articles have been published on the basis and mathematics of the two-photon excitation process and microscopy [24-26]. Here we will describe the basic instrumentation used in our lab for Laurdan GP imaging measurements.

The two-photon source is a Titanium:Sapphire laser pumped by an Argon:ion laser, with an excitation wavelength at 780 nm (Figure 4a). The beam enters the microscope through the epifluorescence port and focuses into the sample through an objective (type, N.A., Zeiss). The red and blue components of the fluorescence are split into two channels by using a dichroic beam splitter (Chroma Technology 470DCXR-BS). Interference filters are placed in the appropriate emission paths to further isolate the 440 and 490 nm region of the emission spectrum (Ealing 490 or Ealing 440, Figure 4b). Two simultaneous 256x256 pixels images are obtained from the sample (image channel-1 and image channel-2) and processed applying the GP formula (eq. 1) to each pixel using the appropriate software (SimFCS, Laboratory for Fluorescence Dynamics, UCI, USA). The resulting image (GP image) can be represented in a histogram of the number of pixels with a given GP where the center of the histogram represents the average GP. A color scale is used for visualizing pixels with different GP values (Figure 5).

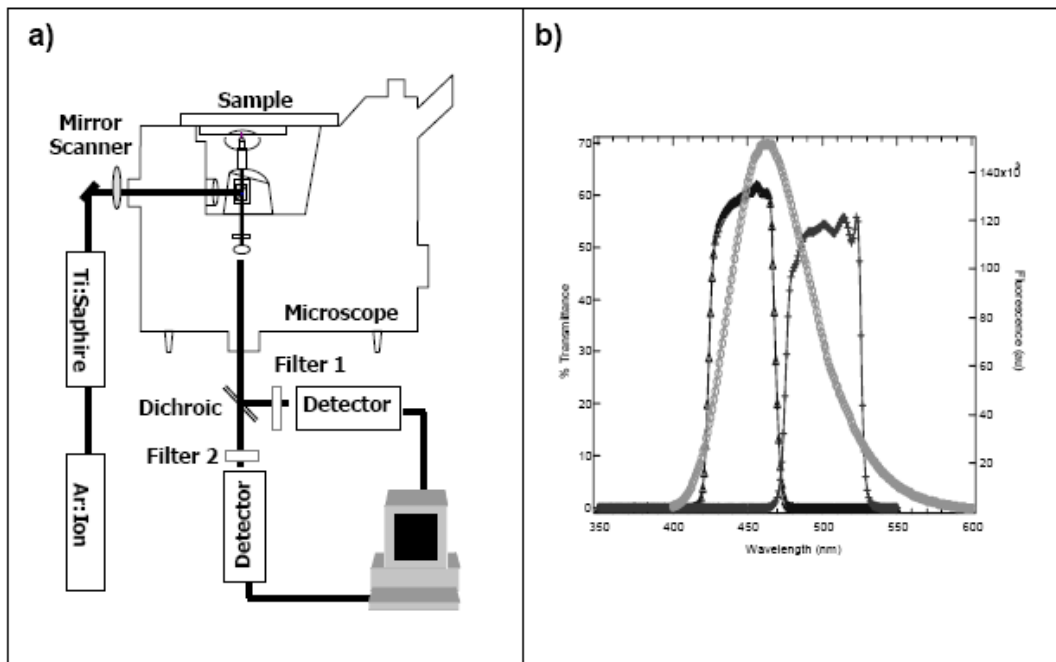


**Fig. 4** GP measurements in the microscope. a) The microscope set up for GP measurements includes the two-photon excitation source (Ti:Sapphire laser pumped by a Argon ion laser), Mirror scanner and two detectors on the emission to register the filtered signal. b). Transmittance of the GP-filters, centered at 440 and 490 nm respectively (in black), overlapped with the emission spectra of Laurdan (in grey). The GP image is generated using the images acquired simultaneously in the two channels.

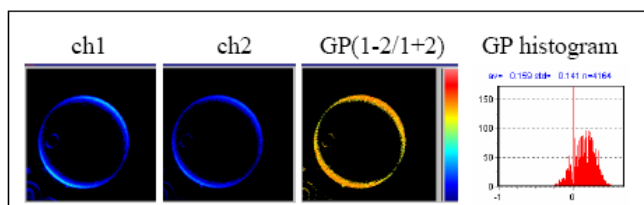


**Fig. 5** GP images are obtain applying the GP function to the images from channel 1 and 2 pixel by pixel. From the GP histogram one can obtain the average GP and the standard deviation of all the pixels in the GP image. Color scale goes from -1 to 1

For membrane studies in the microscope, Giant Unilamellar Vesicles (GUVs) are the lipid model system of choice. Their size, from 10 to 100  $\mu\text{m}$  diameter, permits the visualization of events occurring at the surface and represents a more realistic model for cell membranes. GUVs are fabricated by the electro formation method published by Angelova *et al.* [27] and are widely used in microscopy studies [16,18,28-31]. It is important to consider that contrary to the cuvette studies, where the average behaviour of a vesicle population is measured, in the microscope one or two vesicles are observed at the time, therefore proper statistic methods have to be applied to describe the entire sample.

An important parameter to be considered when Laurdan is used in microscopy studies is the photoselection effect (Figure 6). The transition dipole of Laurdan in phospholipid bilayers is aligned parallel to the acyl chain of the phospholipids (Figure 1a). When vesicles are excited with circular polarized light, a photoselection and thus strong excitation will occur in the plane parallel to the excitation. When illuminating with circular polarized light in the  $x$ - $y$  plane the effect will be particularly stronger in the plane that passes through the center of the vesicle (Figure 6a), and thus it is observed as a bright fluorescent ring (Figure 5). If one observes the top or bottom regions of a spherical lipid vesicle, the photoselection effect will decrease. In addition, this effect will depend upon the state of the lipids. In the liquid-crystalline phase, because of the lipid mobility, some components of the transition dipole can be excited and thus illuminated areas are still detected. Instead, in the gel state, the transition dipole is perpendicular to the excitation plane, and thus dark areas are characteristic on the top and bottom image.

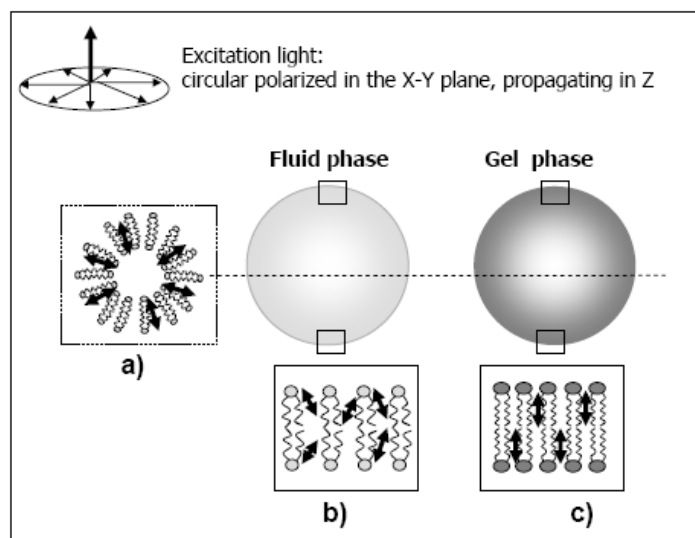


**Fig. 6** Photoselection effect of Laurdan on GUVs. Only the fluorophores that are aligned parallel to the polarization plane of the excitation light will be excited. a) When the excitation light is circularly polarized in the  $x$ - $y$  plane the maximum excitation of the Laurdan molecules can be obtained at the center of the GUV independent of the lipid phase. The photoselection effect exists only at polar region of the vesicle (top and bottom), where the Laurdan molecules are oriented along the  $z$  axis direction in which the excitation light propagates. b) If the lipids are in a fluid phase, a component of the transition dipole of Laurdan is always parallel to the excitation polarization light because of the relatively low lipid order. c) In the gel phase, lipids have a more restricted motion so few molecules) are excited.

The implementation of GP measurements in the microscope provides the tool needed to acquire detailed , information with submicron resolution on the physical characteristics of lipid bilayers. An example is shown in Figure 7. In this case GUVs of DMPC (dimyristoylphosphatidylcholine) were made using a modified version of the electro formation method [15]. The GUV is imaged at different temperatures,

and the average GP value is obtained. The representation of GP vs temperature yields a  $T_m \sim 24^\circ\text{C}$ . This value is in excellent agreement with the previous reported  $T_m$  measured by traditional methods, including Laurdan GP in cuvette, as it was explained for DPPC (Figure 3b). However, no information is supplied by the classical methodology about phenomena occurring at the membrane during the temperature transition. Instead, the GP image at the  $T_m$  shows the presence of some ondulations on the membrane (Figure 7b) that are more evident in the image taken from the top of the vesicle (Figure 7 top-right). This shape change on the surface of the GUV corresponds to the co-existence of lipid in both gel and fluid phases at the transition temperature [18]. The existence of this structure for DMPC was postulated in 1978 by Pownall *et al.* [32]. These authors show that the interaction of apolipoprotein A-I with DMPC vesicles occurs just at the transition temperature. Their conclusion states that this behaviour arises through the formation of a “structural determinant” associated with coexisting gel and liquid crystalline phases. This “determinant” could be either hole or channel defects in the lipid matrix at the borders of coexisting gel and liquid crystalline phases. Thirty years later, we now visualize this “determinant” proving its existence.

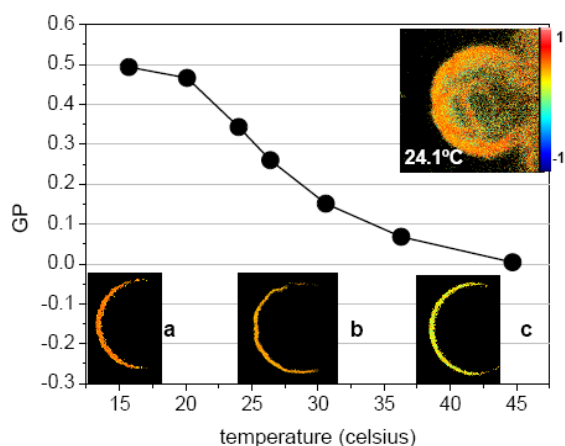


**Fig. 7** Changes in GP with temperature for a DMPC GUV. Closed circles correspond to the average GP value obtained for the whole vesicle. Images show the cross section of the GUV at 15°C (a), 24.1°C (b) and 45°C (c).

Figure on the top right shows the top view of the same GUV at 24.1°C. Same artificial color code scale is being used for all the images.

A more dramatic example showing the power of GP microscopy is shown in Figure 8. Panel 8a of this figure shows the top view GP image of a GUV composed by a mixture of DOPC:DPPC in a 1:1 molar ratio at 23.8 °C. While at this temperature cuvette measurements detect one GP value, the GP image shows that two phases of different GP, i.e., different composition, are coexisting in the same vesicle. When the mixture presents areas with different GP values both the histogram and the GP image can be separated into higher GP and lower GP components. The average GP will be given by

$$GP_{avg} = GP_1 x f_1 + GP_2 x f_2 \quad (2)$$

where  $f_1$  and  $f_2$  correspond to the fractional contributions of the components with higher ( $GP_1$ ) and lower ( $GP_2$ ) GP. The use of adequate computational programs (SimFCS, Laboratory for Fluorescence Dynamics, University of California, Irvine, CA) enables the analysis of the two independent phases at the same time by calculating  $GP_{AVG}$  (average GP from histogram) and the fraction (area of the histogram) of each phase (Figure 8b and c). This set-up has demonstrated to be useful in order to study the interaction of apolipoprotein A-I with binary mixtures and solubilizing lipids preferentially from different domains in equilibrium [16].

By similar experimental designs, this methodology offers the capability to study the influence of temperature on phase separation. An example can be observed in Figure 9, which shows the visualization of the lipid mixture describe above (DOPC:DPPC 1:1 molar ratio) at different temperatures. Above 45°C, one GP value indicates that lipids are organized in a homogeneous phase, but instead below this temperature two GP values are evident and therefore two phases coexist.

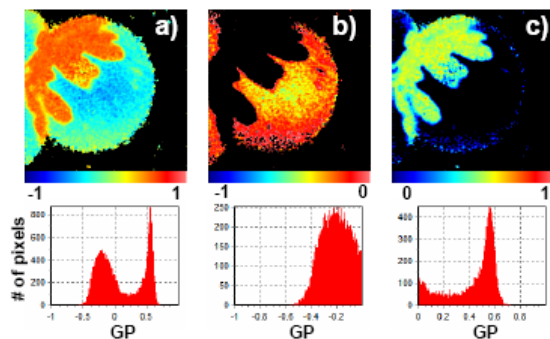


**Fig. 8** Analysis of GP images. a) GP image of a GUV made of DOPC:DPPC 1:1 at 23.8° C. The GP image can be separated in two GP images corresponding to the pixels showing low (b) and high GP values (c). The GP histogram of each image (on the bottom of each image) gives the corresponding average GP value.

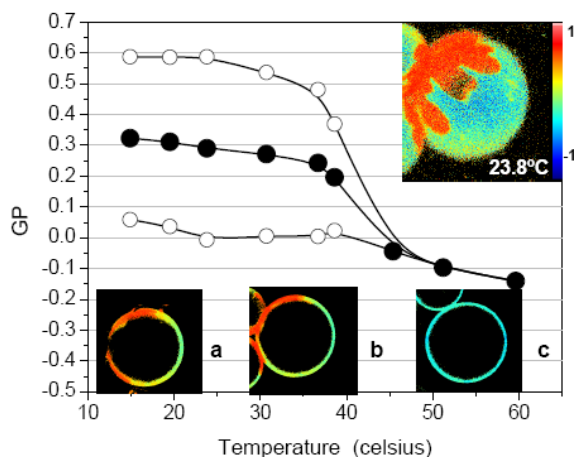


**Fig. 9** Changes in GP with temperature for the 1:1 mixture of DOPC:DPPC. Black dots correspond to the average GP value for the whole vesicle. Images show the cross section of the GUV at 15°C (a), 23.8°C (b) and 60°C (c).

Figure on the top right shows the upper view of the same GUV at 23.8°C. Open circles correspond to the values of the gel (upper values) and fluid (lower values) GP domains in equilibrium. Same artificial color code scale is being used for all the images.

## 5. Final remarks

The implementation of GP measurements in the microscope using two-photon excitation has enormously enhanced the capabilities of this technique. Besides reducing the photo-bleaching of Laurdan, two-photon excitation also provides the confocal sectioning capabilities intrinsic to the two-photon phenomena. Thus, membrane behavior can be studied not only *in vitro* but also *in vivo* where low photodamage and deep penetration is particularly important.

As it is described in this article, GP imaging is particularly useful for studies concerning the coexistence of lipid domains. Lipid rafts have been defined as domains in the membrane enriched in sphingomyelin and cholesterol and its existence *in vivo* is still subject of controversy. Mixtures of phosphatidylcholine, sphingomyelin and cholesterol, so called “raft-like mixtures”, have been used to demonstrate phase separation *in vitro* [20], however the existence of these structures is difficult to be observed *in vivo*. As it was recently shown in macrophages [22], observation of lipid domains coexistence in cells offers an important field for biological studies.

**Acknowledgements:** the support by NIH RR03155 (SS and EG) and Fondecyt 1040573 (GG) are gratefully acknowledged.



## References

- [1] G. Weber, F.J. Farris, *Biochemistry*. 18 (1979) 3075.
- [2] T. Parasassi, G.D. Stasio, A. d'Ubaldo, E. Gratton, *Biophys J*. 57 (1990) 1179.
- [3] T. Parasassi, G. De Stasio, G. Ravagnan, R.M. Rusch, E. Gratton, *Biophys. J.* 60 (1991) 179.
- [4] T. Parasassi, E.K. Krasnowska, L. Bagatolli, E. Gratton, *Journal of Fluorescence* 8 (1998) 365.
- [5] T. Parasassi, E. Gratton, *J. Fluorescence*. 8 (1995) 365.
- [6] T. Parasassi, A.M. Giusti, M. Raimondi, E. Gratton, *Biophys J*. 68 (1995) 1895.
- [7] N. Becerra, L.R.d.l. Nuez, A.L. Zanocco, E. Lemp, G. Gunther, *Colloids and Surfaces A: Physicochem. Eng. Aspects* 272 (2006) 2.
- [8] C.P. Sotomayor, L.F. Aguilar, F.J. Cuevas, M.K. Helms, D.M. Jameson, *Biochemistry* 39 (2000) 10928.
- [9] F.J. Cuevas, D.M. Jameson, C.P. Sotomayor, *Biochemistry* 45 (2006) 13855.
- [10] B.K. Harris FM, Bell JD., *Biochim Biophys Acta*. 1565 (2002) 123.
- [11] J.S. Powalska E, Kinne-Saffran E, Kinne RK, Fontes CF, Mignaco JA, Winter R. , *Biochemistry*. 46 (2007) 1672.
- [12] M. Suwalsky, S. Mennickent, B. Norris, F. Villena, C.P. Sotomayor, *Toxicology in Vitro* 20 (2006) 1363–1369.
- [13] F.M. Harris, S.K. Smith, J.D. Bell, *J Biol Chem*. 276 (2001 ) 22732.
- [14] T. Parasassi, E. Gratton, W.M. Yu, P. Wilson, M. Levi, *Biophysical J*. 72 (1997 ) 2413.
- [15] S.A. Sanchez, L.A. Bagatolli, E. Gratton, T.L. Hazlett, *Biophys. J.* 82 (2002) 2232.
- [16] M.A. Tricerri, J.D. Toledo, S.A. Sanchez, T.L. Hazlett, G. E, A. Jonas, H.A. Garda, *J. Lipid Res*. 46 (2005) 669.
- [17] C. Nicolini, A. Celli, E. Gratton, a.R. Winter., *Biophys J* 91 (2006) 2936.
- [18] L.A. Bagatolli, E. Gratton, *Biophys. J*. 77 (1999) 2090.
- [19] L.A. Bagatolli, S.A. Sanchez, T.L. Hazlett, E. Gratton, *Methods Enzymol*. 360 (2003) 481.
- [20] C. Dietrich, L.A. Bagatolli, Z.N. Volovyk, N.L. Thompson, M. Levi, K. Jacobson, E. Gratton, *Biophysical J*. 80 (2001 ) 1417–1428.
- [21] R. Vest, G. LJ, P. SA, S. E, H. LD, J. AM, B. JD., *Biophys J*. 86 (2004 ) 2251.
- [22] K. Gaus, E. Gratton, E.P.W. Kable, A.S. Jones, I. Gelissen, L. Kritharides, W. Jessup, *Proc. Nat. Acad. Sci*. 100 (2003) 15554.
- [23] S.K. Smith, A.R. Farnbach, F.M. Harris, A.C. Hawes, L.R. Jackson, A.M. Judd, R.S. Vest, S. Sanchez, J.D. Bell, *The Journal of Biol Chem* 276 (2001) 22732–22741.
- [24] P.T.C. So, T. French, W.M. Yu, K.M. Berland, C.Y. Dong, E. Gratton, *Fluorescence Imaging Spectroscopy and Microscopy. Chemical Analysis Series* 137 (1996) 351.
- [25] B.R. Masters, P.T.C. So, E. Gratton, *Fluoresc. Lumin. Probes* (1999) 414.
- [26] G.J. Brakenhoff, M. Muller, R.I. Ghauharali, *J. Microsc.* 183 (1996) 140.
- [27] M.I. Angelova, D.S. Dimitrov, *Faraday Discuss. Chem. Soc.* 81 (1986) 303.
- [28] M.I. Angelova, S. Soleau, P. Meleard, J.F. Faucon, P. Bothorel, *Progr. Colloid Polym. Sci.* 89 (1992) 127.
- [29] K. Bacia, P. Schwille, T. Kurzchalia, *Proc. Natl. Acad. Sci. USA*. 102 (2005) 3272–3277.
- [30] D.A. Brown, *Proc. Natl. Acad. Sci. USA*. 98 (2001) 10517.
- [31] S.L. Veatch, S.L. Keller, *Phys. Rev. Lett.* 89 (2002) 268101.
- [32] Pownall HJ, Massey JB, Kusserow SK, G.A. Jr., *Biochemistry* 17 (1978) 1183.